

## 3D RECONSTRUCTION OF ADOLESCENT SCOLIOTIC TRUNK SHAPE FROM BIPLANAR X-RAYS: A FEASIBILITY STUDY

Laurent Gajny <sup>\*</sup>, Léopold Robichon <sup>\*</sup>, Eleonora Pinto <sup>\*</sup>, Thibault Hernandez <sup>\* †</sup>, Raphaël Vialle <sup>†</sup>, Wafa Skalli <sup>\*</sup>

<sup>\*</sup> Arts et Métiers ParisTech, LBM/Institut de Biomécanique Humaine Georges Charpak,  
151 boulevard de l'Hôpital, 75013 Paris, France  
Corresponding author : laurent.gajny@ensam.eu

<sup>†</sup> Sorbonne University, Department of Paediatric Orthopaedics, Armand Trousseau Hospital, APHP,  
26, avenue du Docteur Arnold-Netter, 75012 Paris, France

**Keywords:** 3D reconstruction, trunk, body-shape, scoliosis, biplanar X-rays.

**Abstract:** *Adolescent idiopathic scoliosis (AIS) is a 3D deformity of the spine detectable by trunk asymmetry. As a decision-aid tool, a body scanner can help assessing non-invasively the external shape of the trunk. However if AIS is diagnosed, additional personalized 3D reconstructions of the spine, rib cage and pelvis are useful to have a complete understanding of the pathology and plan a treatment. For instance, both internal and external geometry are required for computer-aided brace design. Since a body scanner cannot currently guarantee reliable bones reconstruction, low-dose biplanar X-rays (BXR) is a relevant alternative. Indeed, it enables to compute reliable reconstructions of bony structures using validated methods daily used in clinical routine. More recently, 3D body shape reconstruction of asymptomatic subjects from BXR was also proved to be feasible with good accuracy. In order to prevent young scoliotic subjects from multiple examinations, we investigated the feasibility of trunk shape reconstruction from BXR. The proposed method relies on the 3D reconstructions of the spine, rib cage and pelvis priory performed and 10 radio-opaque markers placed on the subject on which we fit a statistical shape model (SSM). This model was built on a training set of 50 asymptomatic and 15 scoliotic female subjects for whom spine, rib cage, pelvis and trunk shape were reconstructed. The trunk shape reconstructions were assessed using the above mentioned method of body shape reconstruction. For the training on scoliotic subjects, this solution was corrected by 100 radio-opaque markers placed on the subjects and detected on the X-rays. During testing, after regression using the SSM, the trunk shape is registered automatically on apparent radiographic contours. Finally, few manual adjustments can be performed. This method has been evaluated on the 15 scoliotic subjects ( $13.7 \pm 1.3$  years,  $Cobb = 23.3^\circ \pm 8.5^\circ$ ) using a leave-one-out procedure. Signed marker-to-surface errors were computed on several trunk regions. The bias was everywhere lower than 0.7mm in absolute value and the standard deviation lower than 6mm. These results are promising and could be improved with a larger database. Thus, this study is a first step toward computer-aided brace design with a single examination.*

## 1. INTRODUCTION

Scoliosis is a clinically apparent pathology by observing the trunk shape. Noticing its asymmetry and/or asymmetry of spinous processes, ribs, and scapulae are determining elements of diagnosis and treatment planning. Currently, the first examination is usually done qualitatively through the clinician's eyes and quantitatively using basic tools such as tape measure or a goniometer.

Optical imaging techniques can help automatizing these measurements through digitalization of the 3D shape of the trunk in a non-invasive way. For instance, [1] demonstrated the reliability of the assessment of the scoliotic trunk using a multihead INSPECK system (INSPECK Inc., Montreal, QC, Canada). More recently in [2], the authors combined statistical analysis with spectral representation of shape for longitudinal analysis of the scoliotic trunk acquired with a similar system. However, at the moment, one cannot guarantee to obtain a reliable estimate of the 3D reconstruction of the spine and rib cage from the external shape without any additional information. Therefore, medical imaging is still needed to have a complete understanding of the pathology and its treatment.

Indeed, for instance, both internal and external geometry of the subject are required for computer-aided design of a brace. Thus, typically, the patient is scanned twice; once using a medical imaging system to assess the internal geometry and once using an optical system for the external geometry. Reducing the number of examination is of great interest for both parts for obvious reasons (comfort, time, money...). In [3], the authors focused on estimating both internal and external geometry from an optical system but the accuracy of the internal geometry has not been quantified yet. In this study, we focus on the use of medical imaging which accurately provides the internal geometry.

Low-dose biplanar X-rays obtained using the EOS system (EOS imaging, Paris, France) is a relevant modality for our purpose since it enables the subject to be in a standing position contrary to CT scan and MRI. Therefore, the trunk shape is not biased by deformations implied by the lying position. In addition, the radiation dose is around 900 times lower comparing to a classical CT scan [4].

Reliable patient-specific reconstruction methods of the spine, rib cage and pelvis from biplanar X-ray for scoliotic subjects are available in the literature [5, 6, 7]. In particular, the spine 3D reconstruction method is daily used in clinical routine. Recently, in [8], the authors have introduced an accurate method of 3D reconstruction of the body shape of asymptomatic subjects from biplanar X-rays. To the best of our knowledge, this study is the first dedicated to an extension of this work onto scoliotic subjects and we focus on the most interesting region of the body shape for scoliotic subjects, *i.e.* the external trunk shape. This study has been lead on 15 female adolescent scoliotic subjects.

## 2. Materials and Methods

### 2.1 Database

After approval of the ethical committee and written informed consent, pairs of biplanar X-rays (EOS imaging, Paris, France) of 65 women of various ages (from 12 to 73 years old) and various morphotypes in the free-standing position [9] have been first collected. Among this population, our testing set is constituted of 15 adolescent female scoliotic subjects (mean age = 13.7 years old  $\pm$  1.3 years; mean Cobb =  $23.3^\circ \pm 8.5^\circ$ ). The other 50 are asymptomatic subjects. The training set is constituted of all the subjects and a leave-one-out procedure is applied during the testing. For validation purpose and model design, 80 to 100 radio-opaque markers were uniformly placed on the scoliotic subjects' skin. Body shape reconstructions of each subject have been assessed using the method [8]. For scoliotic subjects, this solution was enhanced by deforming it using kriging interpolation [10] onto the radio-opaque markers that have been previously detected on the radiographs and reconstructed in 3D using the calibration information. In addition, the 3D spine, pelvis and rib cage of each subjects were reconstructed using validated methods [5, 6, 7]. Finally, humeral head centers were manually identified on both radiographs. Using the calibration information of the EOS cabin, they result on 3D points. After this process, each subject is described in our database with a mesh of the trunk, a simplified model of bony structures and confinement quadrilaterals at 8 predefined level lines (see Figure 1).

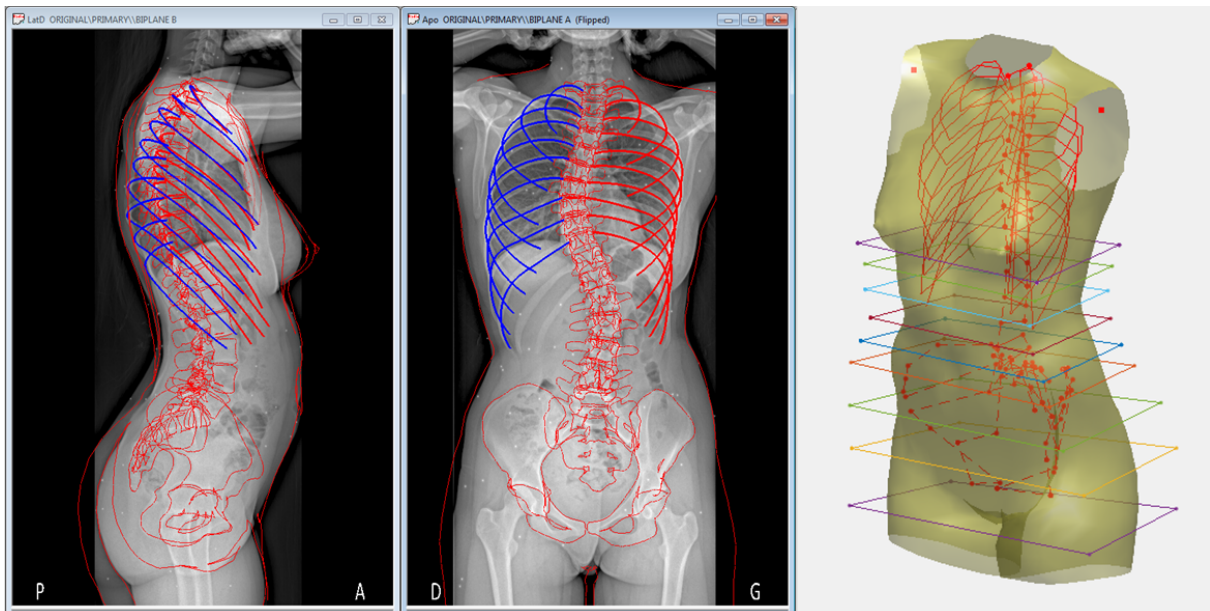


Figure 1. Illustration of the 3D reconstructions done during the training phase of the method (left) and simplification of the obtained information (right) with the 3D mesh of the trunk shape and its descriptors (simplified skeleton and confinement quadrilaterals).

The confinement quadrilaterals are defined as the intersection of the two X-rays incident to the body shape from the X-ray source behind the subject and the two X-rays incident to the body shape from the X-ray source on the right of the subject.

## 2.2 Methods

In this section, the first step of the method to reconstruct the 3D shape of the trunk of a new subject is described. Prior to the acquisition of EOS radiographs, a set of 10 radio-opaque markers are placed on the subject's trunk according to the locations illustrated in Figure 2. In our testing set, these markers are a subset of the larger set of 80 to 100 markers. They will be used in the reconstruction process and their interest will be discussed by also evaluating a marker-less method.

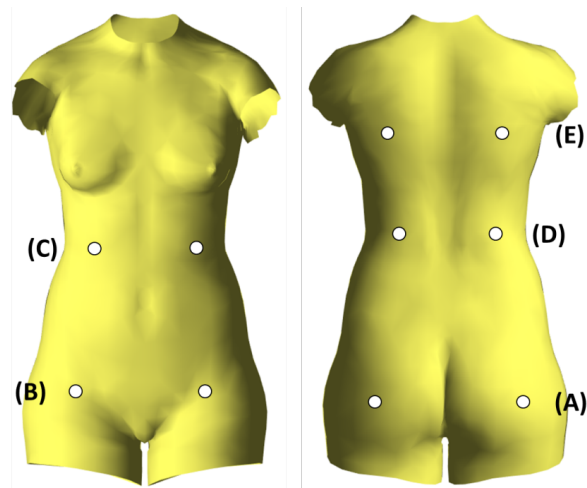


Figure 2. The location of the 10 radio-opaque markers.

A trained user has to reconstruct in 3D the spine from T1 to L5 [5], the rib cage [6], pelvis [7] and to identify the humeral head centers on both views. This enables having a simplified model of the bony structures called skeleton from now. Additional pieces of information are obtained using body shape contours that are extracted automatically from the radiographs using a Gaussian mixture model for a rough background detection and thresholding for segmentation. The intersections of these contours with eight level lines enables to construct the confinement quadrilaterals previously illustrated in Figure 1.

The skeleton and confinement quadrilaterals are then used to infer a first estimate of the 3D external shape of the trunk using a posterior shape model (PSM) as described in [11] and built on our database. This method requires to fix an uncertainty parameter on the predictors which has been fixed in our study at 5mm in each direction (X, Y, Z). Therefore after regression, the closest skeleton in the statistical model to the one used as predictor modulo the uncertainty is obtained. An additional step then deforms the initial 3D mesh of the trunk by applying to it the kriging function [10] that deforms the approximate skeleton onto the one given as predictor of

the PSM.

At this step, we differentiate two methods of trunk reconstruction with and without markers. For the marker-less method, we go directly to the final step. Otherwise, the 3D mesh of the trunk is deformed by kriging [10] to ensure that the radio-opaque marker placed on the subject actually lies on its skin. The detection of the radio-opaque markers on the radiograph is achieved in a semi-automatic way by combining automatic detection and visual checking. The 3D coordinates of the markers' center are deduced using the calibration information. In a final step, the user has the possibility to adjust manually the given solution by moving some control points on the retro-projection of the model onto the radiographs.

### **2.3 Evaluation**

The evaluation has been processed on both methods - with and without markers - on the 15 scoliotic subjects described in the database. A leave-one-out procedure has been applied.

#### **Marker-to-surface distances**

In addition to the 10 markers used in the reconstruction process, the full set of markers placed on the subject were considered as reference points on the body shape of the subject. The markers' radius has been taken into account in the error computation. Signed errors were computed on the trunk regions : posterior thorax, anterior thorax, posterior abdomen, anterior abdomen, buttocks. Breast and shoulders were not considered since they do not provide relevant information for bracing design. An error is positive if the marker is outside the body shape obtained and negative if it is inside.

#### **Anthropometric measurements**

Anthropometric measurements were computed at five horizontal cutting planes (see Figure 3). At each cutting plane, depth, width and circumference of the trunk are computed. Their values are compared with those obtained on the reference trunk shapes that were based on all the radio-opaque markers.

### **3. Results**

Table 1 provides the bias and standard deviation (SD) of signed marker-to-surface errors for each trunk segment for the marker-less method. Table 2 is analogous for the method with 10 markers. The results with and without were within the same range except at the buttocks and the anterior abdomen where the markers yielded to lower errors. With 10 markers, the absolute bias in this case was lower than 1 mm. The 95% confidence interval (considered here as 2SD) is lower than 9.5mm on the whole trunk.

Without and with markers respectively, Tables 3 and 4 provide the mean signed differences and their standard deviation with the reference trunk shapes for each morphometric parameters (C: Circumference, D: Depth, W: Width). Values are given in millimeters and in percentage

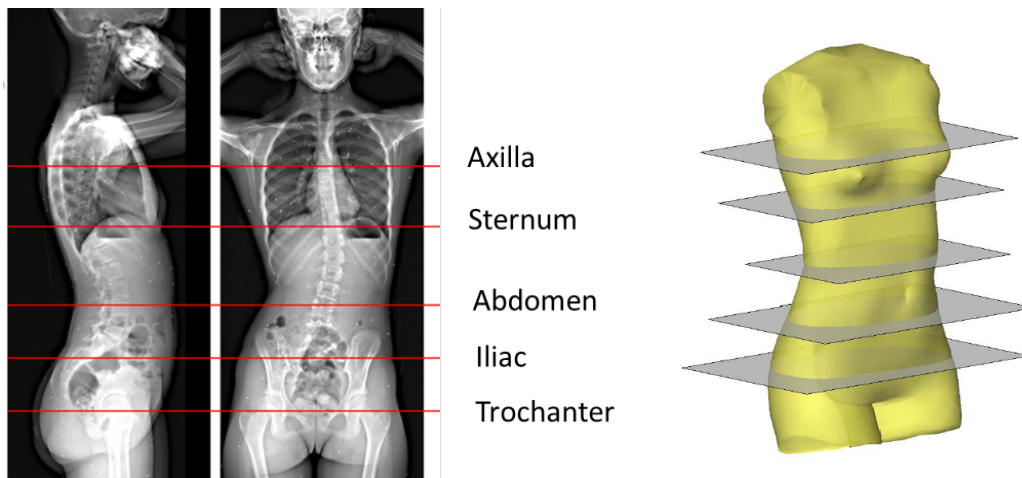


Figure 3. Definition of the cutting planes.

Table 1. Mean signed marker-to-surface error and standard deviation of signed marker-to-surface errors (in mm) for the marker-less method.

| Without Markers | Posterior thorax | Anterior thorax | Posterior abdomen | Anterior abdomen | Thighs & Buttocks |
|-----------------|------------------|-----------------|-------------------|------------------|-------------------|
| Mean SE         | 0.0              | -0.4            | 1.0               | 0.5              | 1.2               |
| SD of SE        | 4.3              | 5.0             | 5.1               | 5.5              | 4.4               |

Table 2. Mean signed marker-to-surface error and standard deviation of signed marker-to-surface errors (in mm) for the method with 10 markers.

| With 10 Markers | Posterior thorax | Anterior thorax | Posterior abdomen | Anterior abdomen | Thighs & Buttocks |
|-----------------|------------------|-----------------|-------------------|------------------|-------------------|
| Mean SE         | 0.5              | -0.6            | 0.8               | 0.1              | 1.0               |
| SD of SE        | 3.9              | 4.5             | 4.7               | 4.6              | 3.6               |

to the reference value. For the method with markers, length and depth computations showed a maximal bias of 3mm and a standard deviation of 5mm around. These values were higher for the computation of circumferences. In absolute value, the mean differences varied from 1 to 8mm and the standard deviation was between 5 and 10 mm. In proportion to the reference values, it was equivalent to a bias in absolute value of at most 1% and a standard deviation between 1 and 4%.

In Figure 4, we illustrate the absolute differences obtained for the circumferences of each subject obtained with the method including the 10 markers. The values are all inferior to 21mm and only two values exceed 15mm.

Table 3. Mean signed difference and standard deviation of signed differences for anthropometric measurements (C: Circumference, D: Depth, W: Width), in mm and in % with regard to the reference value, for the marker-less method.

| Without Markers | Trochanter |    |   | Iliac |   |   | Abdomen |   |   | Sternum |   |    | Axilla |   |    |
|-----------------|------------|----|---|-------|---|---|---------|---|---|---------|---|----|--------|---|----|
|                 | C          | D  | W | C     | D | W | C       | D | W | C       | D | W  | C      | D | W  |
| Mean (mm)       | -2         | -3 | 0 | 4     | 0 | 0 | 8       | 1 | 1 | 4       | 0 | -2 | 1      | 1 | -1 |
| Mean (%)        | 0          | -1 | 0 | 0     | 0 | 0 | 1       | 0 | 1 | 1       | 0 | -1 | 0      | 0 | -1 |
| SD (mm)         | 12         | 4  | 5 | 9     | 3 | 8 | 11      | 4 | 3 | 9       | 3 | 4  | 11     | 8 | 4  |
| SD (%)          | 1          | 1  | 2 | 1     | 1 | 4 | 2       | 2 | 1 | 1       | 1 | 2  | 1      | 3 | 2  |

Table 4. Mean signed difference and standard deviation of signed differences for anthropometric measurements (C: Circumference, D: Depth, W: Width), in mm and in % with regard to the reference value, for the method with 10 markers

| With 10 Markers | Trochanter |    |    | Iliac |   |   | Abdomen |   |   | Sternum |   |    | Axilla |   |   |
|-----------------|------------|----|----|-------|---|---|---------|---|---|---------|---|----|--------|---|---|
|                 | C          | D  | W  | C     | D | W | C       | D | W | C       | D | W  | C      | D | W |
| Mean (mm)       | -4         | -3 | -1 | 2     | 0 | 0 | 3       | 0 | 0 | 2       | 0 | -1 | 3      | 0 | 1 |
| Mean (%)        | 0          | -1 | 0  | 0     | 0 | 0 | 1       | 0 | 0 | 0       | 0 | -1 | 0      | 0 | 0 |
| SE (mm)         | 5          | 3  | 4  | 8     | 3 | 7 | 7       | 3 | 3 | 8       | 4 | 6  | 10     | 5 | 5 |
| SE (%)          | 1          | 1  | 2  | 1     | 1 | 4 | 1       | 1 | 2 | 1       | 1 | 3  | 1      | 2 | 3 |

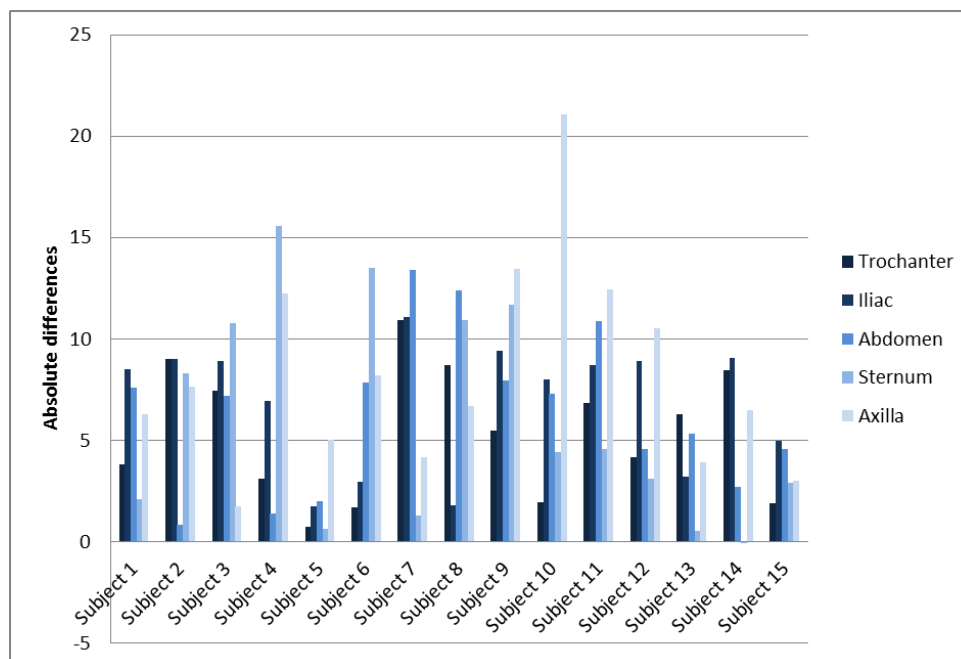


Figure 4. Signed differences obtained for the circumferences of each subject between the method including the 10 markers and the reference method with 80 to 100 markers.

#### **4. Discussion and conclusion**

The aim of this study was to evaluate the feasibility of 3D reconstruction of the scoliotic trunk from biplanar X-rays. A markerless method and a method including 10 radio-opaque markers have been introduced and reconstruction differences with a method based on a large set of markers have been quantified. At the moment, we recommend to use the method with 10 markers as they enable to significantly enhance the shape accuracy. They also enable a better estimate of morphometric parameters (circumferences, depth and width at given cutting planes) that are essential in brace design. Their usefulness can be explained by the choice of their location. There are all located in regions that are not visible on radiographic contours. They also give indications of how the trunk is oriented. Risks of mistakes in identifying the left and right side of the body shape are then decreased.

Enlarging the training database would be a significant improvement of the method. Indeed, a larger database would enable to catch the variability of the scoliotic trunk in a better way, resulting in better pre-positioning of the model and a lower operator dependency (5 minutes of adjustments in average in the final step). Moreover, we expect that a more flexible statistical model would permit to decrease the number of markers. Data collection, particularly of male subjects, is under planning.

A perspective of this work is postural analysis of scoliotic subjects from biplanar X-rays. Once the trunk is reconstructed, the lower limbs and the head can be reconstructed using the method [8] and a full body shape would then permit to compute the gravity line, inertial body segment parameters that are useful for clinicians and researchers in characterizing the pathology.

Overall, the reconstruction errors provided in tables 1 to 4 for the introduced methods are comparable or lower than the one obtained in similar study with other reconstruction methods and on asymptomatic subjects [12, 8, 13, 14] but this study is, to the best of our knowledge, the first dealing with pathological cases. Thus, this study is a first step toward computer-aided brace design with a single examination.

#### **5. Acknowledgment**

The authors deeply thank the ParisTech BiomecAM chair program on subject-specific musculoskeletal modelling and the PROTEOR group (Saint-Apollinaire, France) for their financial support.

#### **References**

- [1] V. Pazos, F. Cheriet, J. Danserau, J. Ronsky, R. F. Zernicke, and H. Labelle. Reliability of trunk shape measurements based on 3-D surface reconstructions. *European Spine Journal*, 16(11):1882–1891, November 2007.



- [2] O. Ahmad, H. Lombaert, S. Parent, H. Labelle, J. Dansereau, and F. Cheriet. Longitudinal Scoliotic Trunk Analysis via Spectral Representation and Statistical Analysis. In *SpringerLink*, pages 79–91. Springer, Cham, October 2016.
- [3] Sasa Cukovic, William R. Taylor, Josette Bettany Saltikov, Zahra Asgharpour, and Nenad Filipovic. Correlation of extrinsic indicators in children suffering from idiopathic scoliosis. In *ESB Sevilla 2017*, pages 0–1, April 2017.
- [4] J. Dubousset, G. Charpak, I. Dorion, W. Skalli, F. Lavaste, J. De Guise, G. Kalifa, and S. Ferey. A new 2D and 3D imaging approach to musculoskeletal physiology and pathology with low-dose radiation and the standing position: the EOS system. *Bulletin De l'Academie Nationale De Medecine*, 189(2):287–297; discussion 297–300, February 2005.
- [5] L. Humbert, J. A. De Guise, B. Aubert, B. Godbout, and W. Skalli. 3D reconstruction of the spine from biplanar X-rays using parametric models based on transversal and longitudinal inferences. *Medical Engineering & Physics*, 31(6):681–687, 2009.
- [6] B. Aubert, C. Vergari, B. Ilharreborde, A. Courvoisier, and W. Skalli. 3D reconstruction of rib cage geometry from biplanar radiographs using a statistical parametric model approach. *Computer Methods in Biomechanics and Biomedical Engineering: Imaging & Visualization*, 4(5):281–295, September 2016.
- [7] D. Mitton, S. Deschênes, S. Laporte, B. Godbout, S. Bertrand, J. A. de Guise, and W. Skalli. 3D reconstruction of the pelvis from bi-planar radiography. *Computer Methods in Biomechanics and Biomedical Engineering*, 9(1):1–5, February 2006.
- [8] A. Nérot, J. Choisne, C. Amabile, C. Travert, H. Pillet, X. Wang, and W. Skalli. A 3D reconstruction method of the body envelope from biplanar X-rays: Evaluation of its accuracy and reliability. *Journal of Biomechanics*, 48(16):4322–4326, December 2015.
- [9] J.-S. Steffen, I. Obeid, N. Aurouer, O. Hauger, J.-M. Vital, J. Dubousset, and W. Skalli. 3D postural balance with regard to gravity line: an evaluation in the transversal plane on 93 patients and 23 asymptomatic volunteers. *European Spine Journal*, 19(5):760–767, May 2010.
- [10] F. Trochu. A contouring program based on dual kriging interpolation. *Engineering with Computers*, 9(3):160–177, September 1993.
- [11] T. Albrecht, M. Lüthi, T. Gerig, and T. Vetter. Posterior shape models. *Medical Image Analysis*, 17(8):959–973, 2013.
- [12] Y.-L. Lin and M.-J. Wang. Constructing 3D human model from front and side images. *Expert Systems with Applications*, 39(5):5012–5018, April 2012.

- [13] S. Zhu, P. Y. Mok, and Y. L. Kwok. An efficient human model customization method based on orthogonal-view monocular photos. *Computer-Aided Design*, 45(11):1314–1332, November 2013.
- [14] S. Zhu and P. Y. Mok. Predicting Realistic and Precise Human Body Models Under Clothing Based on Orthogonal-view Photos. *Procedia Manufacturing*, 3:3812–3819, January 2015.